

REPORT DOCUMENTATION PAGE

Form Approved
OMB No. 0704-0188

Public reporting burden for this collection of information is estimated to average 1 hour per response, including the time for reviewing instructions, searching existing data sources, gathering and maintaining the data needed, and completing and reviewing this collection of information. Send comments regarding this burden estimate or any other aspect of this collection of information, including suggestions for reducing this burden to Department of Defense, Washington Headquarters Services, Directorate for Information Operations and Reports (0704-0188), 1215 Jefferson Davis Highway, Suite 1204, Arlington, VA 22202-4302. Respondents should be aware that notwithstanding any other provision of law, no person shall be subject to any penalty for failing to comply with a collection of information if it does not display a currently valid OMB control number. **PLEASE DO NOT RETURN YOUR FORM TO THE ABOVE ADDRESS.**

1. REPORT DATE (DD-MM-YYYY) 10 July 2016		2. REPORT TYPE Conference Paper with Briefing Charts		3. DATES COVERED (From - To) 02 June 2016 - 10 July 2016	
4. TITLE AND SUBTITLE Fast Computation of High Energy Elastic Collision Scattering Angle for Electric Propulsion Plume Simulation				5a. CONTRACT NUMBER	
				5b. GRANT NUMBER	
				5c. PROGRAM ELEMENT NUMBER	
6. AUTHOR(S) Samuel J. Araki				5d. PROJECT NUMBER	
				5e. TASK NUMBER	
				5f. WORK UNIT NUMBER Q02Z	
7. PERFORMING ORGANIZATION NAME(S) AND ADDRESS(ES) AND ADDRESS(ES) Air Force Research Laboratory (AFMC) AFRL/RQRS 4 Draco Drive Edwards AFB, CA 93524-7160				8. PERFORMING ORGANIZATION REPORT NO.	
9. SPONSORING / MONITORING AGENCY NAME(S) AND ADDRESS(ES) Air Force Research Laboratory (AFMC) AFRL/RQR 1 Ara Drive Edwards AFB, CA 93524-7013				10. SPONSOR/MONITOR'S ACRONYM(S)	
				11. SPONSOR/MONITOR'S REPORT NUMBER(S) AFRL-RQ-ED-TP-2016-135	
12. DISTRIBUTION / AVAILABILITY STATEMENT Approved for public Release; Distribution Unlimited. PA Clearance Number: 16304; Clearance Date: 6/16/2016 The U.S. Government is joint author of the work and has the right to use, modify, reproduce, release, perform, display, or disclose the work.					
13. SUPPLEMENTARY NOTES For presentation at 30th International Symposium on Rarefied Gas Dynamics; University of Victoria, Victoria BC, Canada; 7-10-2016 Prepared in collaboration with ERC; Conference Paper with Briefing Charts					
14. ABSTRACT In the plumes of Hall thrusters and ion thrusters, high energy ions experience elastic collisions with slow neutral atoms. These collisions involve a process of momentum exchange, altering the initial velocity vectors of the collision pair. In addition to the momentum exchange process, ions and atoms can exchange an electron, resulting in slow charge-exchange ions and fast atoms. In these simulations, it is particularly important to accurately perform computations of ion-atom elastic collisions in determining the plume current profile and assessing the integration of spacecraft components. The existing models are currently capable of accurate calculation but are not fast enough such that the calculation can be a bottleneck of plume simulations. This study investigates methods to accelerate an ion-atom elastic collision calculation that includes both momentum- and charge-exchange processes. The scattering angles are pre-computed through a classical approach with ab initio spin-orbit free potential and are stored in a two-dimensional array as functions of impact parameter and energy. When performing a collision calculation for an ion-atom pair, the scattering angle is computed by a table lookup and multiple linear interpolations, given the relative energy and randomly determined impact parameter. In order to further accelerate the calculations, the number of collision calculations is reduced by properly defining an effective elastic collision cross-section that is used to decide if the degree of momentum exchange is insignificant. In the MCC method, the target atom needs to be sampled; however, it is confirmed that initial target atom velocity does not play significant role in typical electric propulsion plume simulations such that the sampling process is unnecessary. With these implementations, the computational run-time to perform a collision calculation is reduced significantly compared to previous methods, while retaining accuracy of the high fidelity models.					
15. SUBJECT TERMS N/A					
16. SECURITY CLASSIFICATION OF:			17. LIMITATION OF ABSTRACT SAR	18. NUMBER OF PAGES 25	19a. NAME OF RESPONSIBLE PERSON D. Bilyeu
a. REPORT Unclassified	b. ABSTRACT Unclassified	c. THIS PAGE Unclassified			19b. TELEPHONE NO (include area code) N/A

Fast Computation of High Energy Elastic Collision Scattering Angle for Electric Propulsion Plume Simulation*

Samuel J. Araki¹

¹ERC Inc., In-Space Propulsion Branch, Air Force Research Laboratory, Edwards Air Force Base, CA 93524, USA

Abstract. In the plumes of Hall thrusters and ion thrusters, high energy ions experience elastic collisions with slow neutral atoms. These collisions involve a process of momentum exchange, altering the initial velocity vectors of the collision pair. In addition to the momentum exchange process, ions and atoms can exchange an electron, resulting in slow charge-exchange ions and fast atoms. In these simulations, it is particularly important to accurately perform computations of ion-atom elastic collisions in determining the plume current profile and assessing the integration of spacecraft components. The existing models are currently capable of accurate calculation but are not fast enough such that the calculation can be a bottleneck of plume simulations.

This study investigates methods to accelerate an ion-atom elastic collision calculation that includes both momentum- and charge-exchange processes. The scattering angles are pre-computed through a classical approach with *ab initio* spin-orbit free potential and are stored in a two-dimensional array as functions of impact parameter and energy. When performing a collision calculation for an ion-atom pair, the scattering angle is computed by a table lookup and multiple linear interpolations, given the relative energy and randomly determined impact parameter. In order to further accelerate the calculations, the number of collision calculations is reduced by properly defining an effective elastic collision cross-section that is used to decide if the degree of momentum exchange is insignificant. In the MCC method, the target atom needs to be sampled; however, it is confirmed that initial target atom velocity does not play significant role in typical electric propulsion plume simulations such that the sampling process is unnecessary. With these implementations, the computational run-time to perform a collision calculation is reduced significantly compared to previous methods, while retaining accuracy of the high fidelity models.

INTRODUCTION

In the plumes of Hall effect thrusters and ion thrusters, ions electrostatically accelerated to high energy can experience elastic collisions with the slow neutral atoms exiting the thrusters. During the collisional process, the high energy ions exchange momentum with their collision partners, and some fraction of the population is deflected at angles greater than the plume divergence. Meanwhile, the elastic collision may involve an exchange of one or more electrons, leading to a slow CEX ion and a high energy atom after each charge-exchange (CEX) process. Therefore, the CEX collision is considered as a subset of elastic collision, and we call the elastic collision without an exchange of charge a MEX collision. Proper modeling of these collisions is particularly important in accurately determining the plume current profile and assessing the integration of spacecraft components as well as the thruster life and long duration performance; the slow CEX ions are prone to electric fields that direct the ions toward the spacecraft and thruster components, resulting in contamination through sputtering and deposition after gaining significant energies.

The elastic collision between high energy ions and slow atoms has been approximated by a few different methods. In a particle-in-cell (PIC) model developed by Oh [1], simple models were employed; the elastic collision was treated as isotropic scattering whereas the CEX collision was handled without any exchange of momentum. More recently, the elastic collision has been calculated by a detailed model that solves the classical scattering equation with a precise interatomic potential [2, 3, 4]. This method provides much more accurate scattering characteristics necessary for plume simulations. However, the numerical integration of classical scattering equation is computationally expensive such that the collision calculation can be a bottleneck to a massive particle simulation. An alternative method is to use a curve-fit representation of a center-of-mass (CM) differential cross-section to determine post-collision particle velocities [5, 6]. This method is much faster than the direct numerical integration. However, it is limited to the energy

*Distribution A: Approved for public release; Distribution Unlimited. PA Clearance No. 16304

that the differential cross-section is provided at. At the exit plane of the Hall thruster, ions do not necessarily have the energy equivalent to the potential difference between a cathode and an anode, as they are created at different locations along the channel. Furthermore, their energies after the first collision are always reduced significantly for the case of large angle scattering. Therefore, the collision calculation method does not provide accurate collision characteristics for every particle within the plume.

The objective of this research is to develop a fast and accurate method to compute the scattering angle for an elastic collision between high energy ions and slow atoms. Instead of using the experimentally determined differential cross-section, the CM differential cross-section can be numerically computed from the classical theory at any incident ion energy. By determining an applicable range of impact parameters for a given energy and formulating a two-dimensional array of scattering angles as functions of impact parameter and energy, the scattering angle can be quickly obtained by a table lookup. This paper provides the detail of the table formulation and compares its performance with other methods. Although the paper deals primarily with $\text{Xe}^+ + \text{Xe}$ collision, the same concept can be applied to collisions between other species.

NUMERICAL METHOD FOR COLLISION CALCULATION

Classical Scattering Model

Two classes of collision models, Monte Carlo Collision (MCC) and Direct Simulation Monte Carlo (DSMC) models, are commonly used for particle simulations of plasma with collisions. Both models involve determination of scattering angles and alteration of particle velocity vector when applying elastic collisions to particles. Phenomenological models such as variable hard-sphere (VHS) model [7] have been successfully used in simulations of rarefied gas. These models are designed to reproduce the property of real gases by choosing adjustable parameters to match the experimental data. Furthermore, simple scattering characteristics allow fast computation of post-collision velocity vectors. In plumes of spacecraft propulsion devices, the background gas density rapidly reduces away from the thrusters so that at most a few elastic collision events per incident particle would take place. Therefore, the unrealistic scattering characteristics employed in the phenomenological models would not permit in accurate determination of the plume current profile. The scattering characteristics of ions and neutral atoms can be obtained more precisely through the classical approach, integrating the interatomic force between the collision pair along the incident particle's trajectory as shown in Figure 1. The deflection angle in the center of mass (CM) frame, χ , is expressed as

$$\chi(b, E_r) = \pi - 2b \int_{R_m(b, E_r)}^{\infty} \frac{dr}{r^2 [1 - b^2/r^2 - V(r)/E_r]^{\frac{1}{2}}} \quad (1)$$

where b is the impact parameter, r is the internuclear distance, $V(r)$ is the interatomic potential, and E_r is the relative energy. The classical turning point or the minimum distance of approach, R_m , is calculated by finding the largest root of the equation.

$$1 - b^2/R_m^2 - V(R_m)/E_r = 0 \quad (2)$$

Equation (1) and (2) may be evaluated analytically if the potential function $V(r)$ is simple. However, this is often not the case for a function that closely approximates the real interaction potential. Computing Equation (1) with direct numerical integration can be difficult since the denominator approaches zero in the limit of $r = R_m$. Instead, Equation (1) is solved by applying the Gauss-Mehler formula [8].

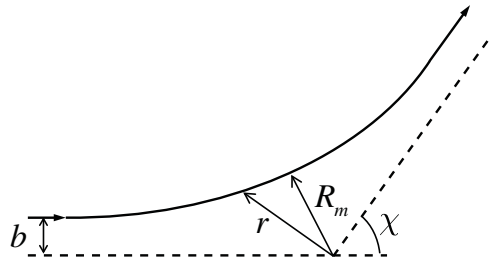


FIGURE 1. Classical scattering trajectory.

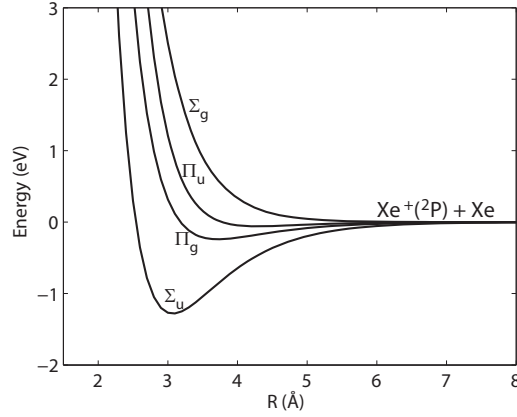


FIGURE 2. Spin-orbit free interaction potential energy curve for $\text{Xe}^+(^2\text{P})+\text{Xe}$ calculated by Paidarova and Gadea [10].

The interaction potentials for $\text{Xe}^+ + \text{Xe}$ collisions have been calculated with *ab initio* quantum chemistry [9, 10, 11]. In the computational model, four spin-orbit free potentials, Π and Σ potentials with the *gerade* (g) and the *ungerade* (u) states, calculated by Paidarova and Gadea are used [10]. These potentials are shown in Figure 2. Chiu et al. [12] verified that the scattering results are not affected significantly by using the full spin-orbit potentials. The averaged (u,g) pairs of the spin-orbit free potentials are fitted using Morse potential form and the fitting parameters are given in Ref. 12.

$$V_{\text{avg}}(r) = D_e(e^{2b(r_e-r)} - 2e^{b(r_e-r)}) \quad (3)$$

The statistical weights for Σ and Π potentials, d_Σ and d_Π , are 1/3 and 2/3, respectively.

Figure 3 shows the center of mass deflection angle as a function of impact parameter for different center of mass energies. Note that $E_r = 150$ eV roughly corresponds to the laboratory (LAB) frame incident ion energy ($E = 300$ eV) typically seen in a Hall-effect thruster plume. The deflection function for $E_r = 0.5$ eV has a small minimum at $b \approx 4.9$ Å, which gives a rainbow singularity in the differential cross-section at the rainbow angle corresponding to the minimum deflection angle. Also, the deflection function becomes discontinuous at the critical angle at even lower energies (i.e. orbiting singularity). These singularities are not realistic, and quantum scattering has to be considered [13, 14]. However, at high energies, the deflection is mostly affected by the repulsive part of the potential at short-range so that the deflection function barely has a minimum. In this regime, the classical scattering model is sufficiently accurate to approximate ion-atom collision behavior [14]. For all the energies, the CM scattering angle approaches zero as $b \rightarrow \infty$, however, it never actually reaches zero. This implies that the total collision cross-section is unbounded unless the quantum scattering theory is considered. In applying the classical model, it is necessary to provide a cut-off impact parameter or deflection angle [7]. The cut-off impact parameter is chosen from the deflection functions at different energies as discussed hereinafter.

Total Cross-Section

Charge exchange collision cross-sections have been measured experimentally and fitted to a simple logarithmic formula by Miller et al. [15].

$$\sigma_{\text{CEX}} = 87.3 - 13.6 \log(E) \quad (4)$$

Equation (4) generally agrees well with previous experimental measurements and has been verified theoretically by a semi-classical calculation. The semi-classical calculation involves an integration of charge-exchange probability, P_{CEX} (see Figure 4), evaluated from the elastic phase shifts for the two states. At small impact parameters, P_{CEX} oscillates rapidly between 0 and 1, and the average value of 0.5 is typically used in models. At larger impact parameters, its maximum value in the oscillation starts to decrease due to the stronger interaction of Σ potentials. However, the deflection is close to zero in this regime such that precise approximation of charge exchange probability is not necessary. For this reason, previous computational models have approximated elastic collision cross-section to be twice the CEX cross-section, i.e. $\sigma_{\text{total}} = 2\sigma_{\text{CEX}}$, and used $P_{\text{CEX}} = 0.5$ [2, 3].

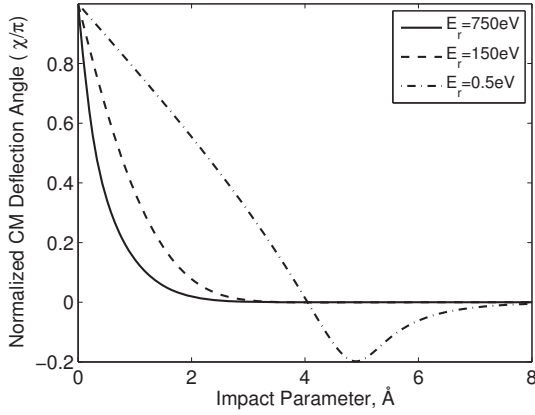


FIGURE 3. Deflection functions computed at different CM energies.

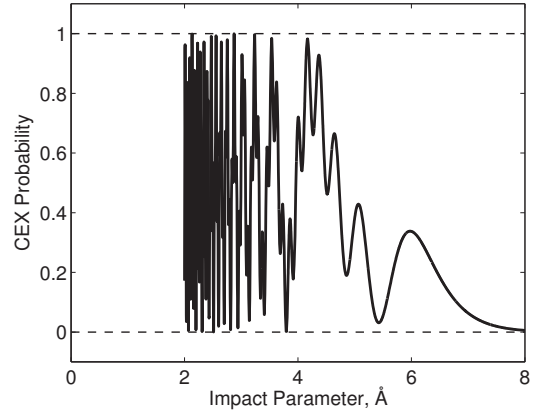


FIGURE 4. Charge-exchange probability for a relative energy of 150 eV.

Larger cross-section leads to more collision calculations due to the increased collision probability. Calculation of post-collision velocity involves computation of scattering angle and multiple coordinate transformations between LAB and CM frames and between pre- to post-collision velocity reference frames. Performing these calculations for a number of collision pairs can be computationally expensive. Therefore, the computational cost can be reduced by simply skipping the collision calculation for collision pairs that do not experience significant momentum transfer. Let us define an effective elastic collision cross-section, σ_{el} , which acts as a limit that deflection can occur. Note that the CEX process may still occur when the impact parameter is within σ_{el} . The cross-section can be obtained by choosing the cut-off impact parameter from the deflection functions at different energies. Finding the impact parameter corresponding to the cut-off deflection angle of 1° and calculating the corresponding cross-section by $\sigma = \pi b^2$, σ_{el} can be fitted to a logarithmic formula.

$$\sigma_{el} = 62.3 - 13.4 \log(E) \quad (5)$$

The cut-off deflection angle can be chosen to be other than 1° , but a larger angle would result in a loss of accuracy while reducing the computational cost. The classical theory is no longer accurate within the glory singularity regime such that a smaller cut-off angle would not necessarily increase the accuracy. At the LAB energy of 300 eV, $\sigma_{total} = 107.2 \text{ \AA}^2$ and $\sigma_{el} = 29.1 \text{ \AA}^2$; therefore, roughly 73% of collision calculation can be cut.

Differential Cross-Section

Although the differential cross-section is not used anywhere in the collision calculation, it is covered herein to facilitate later discussions. The differential cross-section is useful in verifying the implementation as it can be obtained by (a) numerically evaluating from theory and (b) applying collisions and sampling particles in the code. Unlike the deflection function shown in Figure 3, the differential cross-section includes both the MEX and CEX collision effect. Once the deflection angles at different impact parameters are computed by Equation (1), the differential cross-section can be determined by the following equation.

$$I_{CM}(\chi, E_r) = \left. \frac{d\sigma(\chi)}{d\Omega} \right|_{CM} = \left| \frac{b}{\sin\chi(d\chi/db)} \right| \quad (6)$$

Here, $d\chi/db$ can be approximated by using first order difference equations. Taking into account backscattered CEX ions, the differential cross-section can be rewritten as [12]

$$I'_{CM}(\chi) = (1 - P_{CEX}(\chi))I_{CM}(\chi) + P_{CEX}I_{CM}(\pi - \chi) \quad (7)$$

The first and second terms on the right-hand side of Equation (7) denote the MEX and CEX collision contributions to the total differential cross-section, respectively. If the collision partners have equal mass and the target particle is

stationary, the CM differential cross sections can be converted into the LAB reference frame by [2]

$$\left. \frac{d\sigma}{d\Omega} \right|_{\text{LAB}} = I'_{\text{CM}}(\chi) 4 \cos(\chi/2) \quad (8)$$

For the CEX collision, the LAB differential cross section is calculated by replacing χ with $\pi - \chi$ in Equation (8). The high probability in small angle scattering for the energy of interest leads to large differential cross-sections at extreme angles of 0° and 90° as a result MEX and CEX collisions, respectively.

Formulation of Matrix for Table Lookup

In determining the scattering angle by computing Equation (1), the Gauss-Mehler formula works significantly better than the direct numerical integration with respect to speed and accuracy. However, performing the calculation for a number of particles on the fly can be computationally expensive. A much more attractive way is to pre-compute the scattering angles for ranges of energies and impact parameters and perform a linear interpolation of the stored scattering angles. In the 2-dimensional array of scattering angles, the energy values are distributed uniformly within the minimum and maximum CM energies, defined as E_{\min} and E_{\max} , respectively.

$$E_j = E_{\min} + j \Delta E, \quad 0 \leq j \leq N_E - 1 \quad (9)$$

where $\Delta E = (E_{\max} - E_{\min})/(N_E - 1)$ and N_E is the number of energy values. Each discrete energy value, E_j , is associated with a cut-off impact parameter, b_{\max} , defined by the effective elastic cross-section given in Equation (5). The minimum impact parameter is simply zero so that the impact parameter values to evaluate the scattering angle are uniformly distributed between 0 and b_{\max} .

$$b_i = i b_{\max}/(N_b - 1), \quad 0 \leq i \leq N_b - 1 \quad (10)$$

The scattering angle, $\chi_{i,j}$, is evaluated for every combination of b_i and E_j and is stored in the 2-dimensional array. In order to ensure a smooth variation of scattering angle near the cut-off impact parameter, χ is forced to be zero at b_{\max} .

For a given pair of particles, the CM energy is not necessarily at the values used to formulate a table. Therefore, the scattering angle is determined by interpolating to the values for the collision pair. First, the fractional energy index, j_f , for the table is obtained such that the CM energy, E_p , is bounded by E_j and E_{j+1} .

$$j_f = (E_p - E_{\min})/\Delta E \quad (11)$$

The integer value of j_f is used as the energy index, i.e. $j = \text{int}(j_f)$, and the weight for linear interpolation is simply given as $w_j = j_f - j$. Since the maximum impact parameter differs for every energy, the fractional impact parameter indices are not the same for E_j and E_{j+1} .

$$i_{f,j} = b_p/\Delta b_j \quad (12)$$

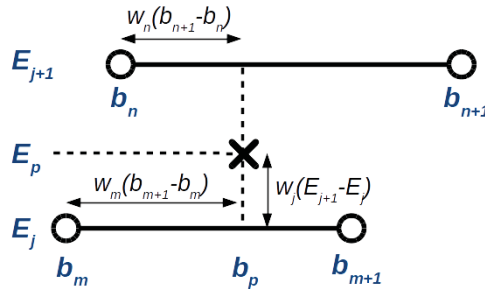


FIGURE 5. Illustration of the interpolation process used to determine scattering angle. Indices of m and n are used in place of i_j and i_{j+1} , respectively.

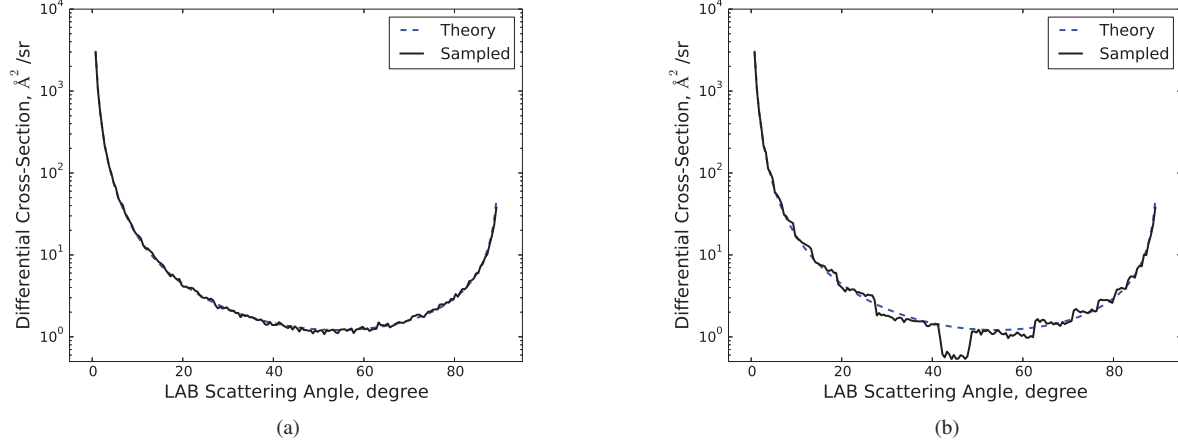


FIGURE 6. LAB differential cross-section computed from theory and by sampling particles from the code. The impact parameter values in the table is distributed (a) uniformly in b and (b) uniformly in b^2 .

Indices and weights for i_j and i_{j+1} are obtained similarly as the case of energy. Finally, the scattering angle is obtained by performing three linear interpolations.

$$\begin{aligned}
 \chi(b_p, E_j) &= (1 - w_{i_j})\chi(b_{i_j}, E_j) + w_{i_j}\chi(b_{i_{j+1}}, E_j) \\
 \chi(b_p, E_{j+1}) &= (1 - w_{i_{j+1}})\chi(b_{i_{j+1}}, E_{j+1}) + w_{i_{j+1}}\chi(b_{i_{j+1}+1}, E_{j+1}) \\
 \chi(b_p, E_p) &= (1 - w_j)\chi(b_p, E_j) + w_j\chi(b_p, E_{j+1})
 \end{aligned} \tag{13}$$

The interpolation process is also illustrated in Figure 5.

Tabulation of scattering angle and use of a look-up table have also been implemented by Sharipov and Strapasson [16]. However, the distribution of impact parameter is different in that they used uniform distribution of b^2 instead of b . Their approach ensures equal probability that the impact parameter lie within every bin (e.g. between b_j and b_{j+1}). Unlike their application, the most important collision within the spacecraft plume is at high energy such that the deflection function is roughly monotonically decreasing with larger impact parameters (see Figure 3). In order to capture the plume current profile correctly, it is necessary to resolve the small impact parameter region where large angle scattering occurs. Due to the steeper slope in deflection function as b approaches $b = 0 \text{ \AA}$, a uniform distribution in b^2 results in less accurate scattering angles near the region. Therefore, a uniform distribution in b is chosen to improve the accuracy as b approaches $b = 0 \text{ \AA}$ for a given number of impact parameter in the table. Figure 6 compares the differential cross-section computed from the code by sampling particles after a single elastic collision. In constructing a table to determine scattering angles, 50 impact parameter values are used ($N_b = 50$). It is readily seen that the uniform distribution of b agrees much better with the theory than a uniform distribution of b^2 . The sampled differential cross-section approaches the theoretical one as N_b is increased.

Implementation in Monte Carlo Collision Method

Figure 7 shows the flowchart of the elastic collision calculation algorithm, utilizing three different cross-sections (i.e. σ_{total} , σ_{el} , and σ_{CEX}) given in Equation (4) and (5). The total cross-section, σ_{total} , can be arbitrarily chosen as long as it is greater than $\sigma_{\text{CEX}} + 0.5\sigma_{\text{el}}$. The case shown in Figure 7 assumes that $\sigma_{\text{total}} = 2\sigma_{\text{CEX}}$ such that $P_{\text{CEX}} = 0.5$ for any value of impact parameter. For a case where $\sigma_{\text{total}} \neq 2\sigma_{\text{CEX}}$, P_{CEX} for $b > b_{\text{max}}$ needs to be refined such that $\sigma_{\text{CEX}} = P_{\text{CEX},1}\sigma_{\text{el}} + P_{\text{CEX},2}(\sigma_{\text{total}} - \sigma_{\text{el}})$ is maintained, where $P_{\text{CEX},1} = 0.5$ covers $b \leq b_{\text{max}}$ and $P_{\text{CEX},2}$ is the adjustable parameter that covers $b > b_{\text{max}}$.

The Monte Carlo collision routine involves a step to determine whether the collision between the collision pair occurs by comparing a collision probability, P_{total} , with a random number, U_1 , between 0 and 1,

$$P_{\text{total}} = 1 - \exp(-\gamma n_0 \sigma_{\text{total}} v_{\text{rel}} \Delta t) \tag{14}$$

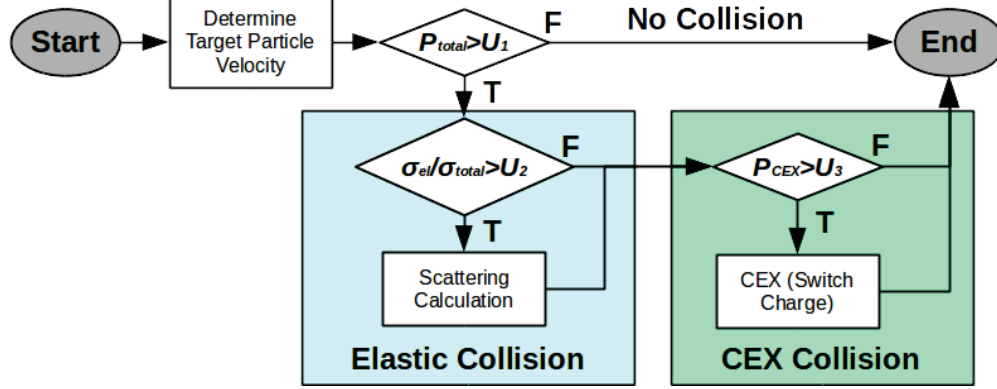


FIGURE 7. Simplified flowchart of elastic collision calculation algorithm in context of MCC collision method.

where γ is the collision factor that is 1 for the same species pair and 0.5 for unlike species pair, n_0 is the target gas density, v_{rel} is the relative speed between the collision pair, and Δt is the time-step. If $P_{total} > U_1$ is satisfied, the next step involves determining if the scattering angle is significant enough to be computed. The impact parameter for the collision event is $b = b_{max} \sqrt{U_2}$ where U_2 is another random number. If the impact parameter is smaller than the radius of effective elastic collision cross-section (i.e. $b < \sqrt{\sigma_{el}/\pi}$), then the post-collision velocity is computed using the impact parameter. The post collision velocity calculation is done in the CM frame so that it involves multiple coordinate transformations and a scattering angle calculation by a table lookup as discussed in the previous sections. After the elastic collision calculation, the velocity vector is switched if the third random number, U_3 , is smaller than the charge exchange probability.

The overall cost of the collision calculation is minimized if the smallest possible total cross-section is used, as it leads to the smallest value for P_{total} according to Equation (14) such that the chance of experiencing a collision is minimized. In this study, $\sigma_{total} = 2\sigma_{CEX}$ is chosen instead of $\sigma_{CEX} + 0.5\sigma_{el}$ due to the simplicity in implementation, but the refinement can be done easily with a slight modification.

COMPARISON OF PERFORMANCE

The collision calculation methods are compared in context of their performance in speed. In this study, approximately 1, 146, 700 particles are injected into the domain at a speed of 19, 920 m/s (270 eV). The target gas density is set to a very high value such that all the particles undergo one elastic collision per step (i.e. $P_{total} \approx 1$). The calculation is repeated 100 times, and only the time to perform the collision calculation is reported. We used the implementation in COLISEUM [5] as a baseline and incrementally added improvements including (1) a lookup table and (2) an effective elastic collision cross-section. Lastly, we performed the calculation assuming (3) a stationary background target gas, after implementing the two improvements. All of these implementations were checked to assess their correctness by sampling the particle's scattering angle and comparing with the differential cross-section. The current model with the MCC method samples the target particle velocity assuming the Maxwellian distribution. However, the actual distribution in a plume should be close to the one obtained by tracing neutral particles leaving the thruster exit face at a cosine distribution. Nevertheless, the target particle speed is so slow that, after becoming an CEX ion, its particle

TABLE 1. Performance comparison of collision calculation methods. (1), (2), and (3) are incrementally implemented into the code.

	Wall Time, s	% Baseline
Baseline	61.67	100.0
(1) Lookup Table	45.75	74.2
(2) Effective Elastic Collision σ	36.21	58.7
(3) Stationary Background Gas Assumption	17.63	28.6

motion is steered by the electric field, and the particle's initial velocity does not affect its trajectory significantly. Note that this would not be an issue in the DSMC method as it does not require any sampling from a fluid property but rather requires a selection of target particles from a simulation particle list. It should also be noted that the assumption of stationary target particle only works for the case where the electric potential within the plume is significantly higher than the target gas energy, which is often the case for electric propulsion plumes. The validity of the stationary gas assumption in a plume simulation is further discussed in the next section.

Table 1 shows the wall time for the collision calculation and its percentage relative to the baseline method. While the baseline method is nearly optimized in sampling the scattering angles from the differential cross-section, the acceptance-rejection routine used in the baseline method was still significantly more expensive compared to a simple lookup from a table, as indicated by the percent reduction in wall time of 25.8 percent. Furthermore, with an implementation of σ_{el} , an additional 15.5 percent reduction in wall time was achieved. At this point, the most expensive operation was to sample the target particle velocity from a Maxwellian distribution, even though this would not lead to a more accurate solution in any way from the stationary background gas assumption. By skipping the sampling and assuming a target gas velocity of zero, another 30.1 percent of collision calculation time was cut. The overall reduction of the collision calculation was 71.4 percent compared to the baseline implementation.

EFFECT OF TARGET NEUTRAL ATOM VELOCITY

The pre-collision target atom velocity distribution has a great impact on a post-collision CEX ion angular distribution especially for elastic collisions that involve small degree of momentum transfer. As a result, the differential cross-section at larger LAB scattering angles is smeared out and approaches the pre-collision target atom distribution. Figure 8 (a) compares the LAB differential cross-section obtained for different pre-collision target atom temperature. It is clearly seen that the CEX population with large angle deflection is reduced significantly. However, the change in the differential cross-section is only attributed to slow ions having post-collision velocities similar to their initial velocities. Since the slow ions are easily affected by the electric field, the change in the differential cross-section does not provide any information to what degree the target atom velocity distribution affects the plume simulation results.

In order to confirm that the stationary target gas assumption is reasonable in plume simulations, the speed distribution is sampled from ion population after a single elastic collision event. Figure 8 (b) shows the speed distribution for target gas temperatures of 300 K and 0 K. For almost the entire range of the kinetic energy, the distribution function is nearly the same, except for the fluctuation due to the statistical noise. The only energy range that is significantly affected by the target gas temperature is below 0.2 eV, indicating CEX ion trajectories are not affected by the assumption as long as there is a potential difference between a cell that the slow ion resides in and neighboring computational cells that is more than 0.2 V. This is often the case in electric propulsion plumes, especially near the thruster exit where the CEX ions are mostly generated.

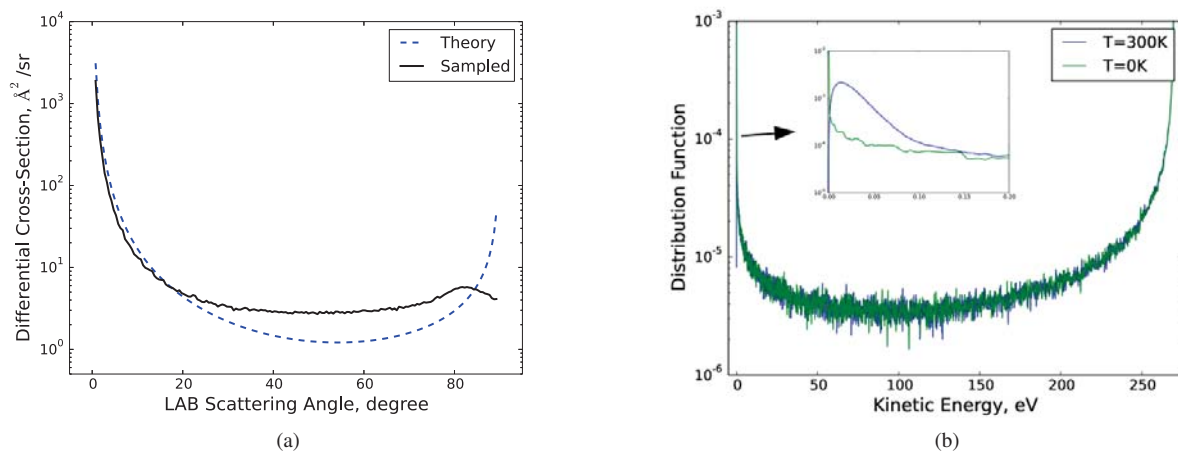


FIGURE 8. (a) LAB differential cross-sections. The theoretical differential cross-section is computed for stationary target gas (0 K) whereas the one sampled from particles are obtained with initial target particle distribution of Maxwellian at 300 K. (b) Sampled post-collision speed distribution for target gas temperature of 300 K and 0 K.

CONCLUSION

This study has investigated methods to accelerate an ion-atom elastic collision calculation that includes both momentum- and charge-exchange processes for electric propulsion plume simulations. The scattering angles are pre-computed through a classical approach with *ab initio* spin-orbit free potential and are stored in a two-dimensional array as functions of impact parameter and energy. When performing a collision calculation for an ion-atom pair, the scattering angle is computed by a table lookup and multiple linear interpolations, given the relative energy and randomly determined impact parameter. In order to further accelerate the calculations, the number of collision calculations is reduced by properly defining an effective elastic collision cross-section, σ_{el} , that is used to determine if the degree of momentum exchange is insignificant. The effective elastic cross-section is a function of energy and is used to obtain the maximum impact parameter in formulating the array for a lookup table. In the MCC method, the target atom needs to be sampled; however, it is confirmed that initial target atom velocity does not play any significant role in typical electric propulsion plume simulations such that the sampling process is unnecessary. With these implementations, the computational run-time to perform a collision calculation is reduced by 71.4 percent compared to the method implemented in COLISEUM, while improving accuracy for energies that the previous method was not optimized for.

REFERENCES

- [1] D. Oh, "Computational modeling of expanding plasma plumes in space using a PIC-DSMC algorithm," Ph.D. thesis, Massachusetts Institute of Technology, Cambridge, MA 1997.
- [2] I. Mikellides, I. Katz, R. Kuharski, and M. Mandell, *Journal of Propulsion and Power* **21**, 111–118 (2005).
- [3] I. D. Boyd and R. A. Dressler, *Journal of Applied Physics* **92**, 1764–1774 (2002).
- [4] S. J. Araki and R. E. Wirz, *IEEE Transactions on Plasma Science* **41** (2013).
- [5] M. K. Scharfe, J. W. Koo, and G. Azamia, "DSMC implementation of experimentally-based $Xe^+ + Xe$ differential cross sections for electric propulsion modeling," in *AIP Conference Proceedings*, Vol. 1333 (AIP, 2011), pp. 1085–1090.
- [6] P. N. Giuliano and I. D. Boyd, *Physics of Plasmas* **20** (2013).
- [7] G. A. Bird, *Molecular Gas Dynamics and the Direct Simulation of Gas Flows* (Clarendon Press, Oxford, 1994).
- [8] F. J. Smith, *Physica* **30**, 497–504 (1964).
- [9] M. Amarouche, G. Durand, and J. P. Malrieu, *Journal of Chemical Physics* **88**, 1010–1018 (1988).
- [10] I. Paidarova, *Chemical Physics* **274** (2001).
- [11] J. A. S. Barata and C. A. N. Conde, *IEEE Transaction on Nuclear Science* **52**, 2889–2894 (2005).
- [12] Y.-H. Chiu, R. A. Dressler, D. J. Levandier, C. Houchins, and C. Y. Ng, *Journal of Physics D: Applied Physics* **41**, p. 165503 (2008).
- [13] M. S. Child, *Molecular Collision Theory* (Academic Press Inc., London, 1974).
- [14] I. Katz, G. Jongeward, V. Davis, M. Mandell, I. Mikellides, I. Boyd, A. Arbor, K. Kannenberg, and D. King, "A Hall Effect Thruster Plume Model Including Large-Angle Elastic Scattering," in *37th AIAA/ASME/SAE/ASEE Joint Propulsion Conference & Exhibit* (Salt Lake City, Utah, 2001), pp. 1–16, AIAA 2001–3355.
- [15] J. S. Miller, S. H. Pullins, D. J. Levandier, Y.-H. Chiu, and R. A. Dressler, *Journal of Applied Physics* **91**, 984–991 (2002).
- [16] F. Sharipov and J. L. Strapasson, *Physics of Fluids* **24**, 1–6 (2012).

Fast Computation of High Energy Elastic Collision Scattering Angle for Electric Propulsion Plume Simulation

Samuel J. Araki¹

ERC Inc, Air Force Research Laboratory
Edwards Air Force Base, CA USA¹

30th International Symposium on Rarefied Gas Dynamics,
University of Victoria, July 10-15th, 2016

Distribution A: Approved for Public Release; Distribution Unlimited
PA Clearance No. 16304

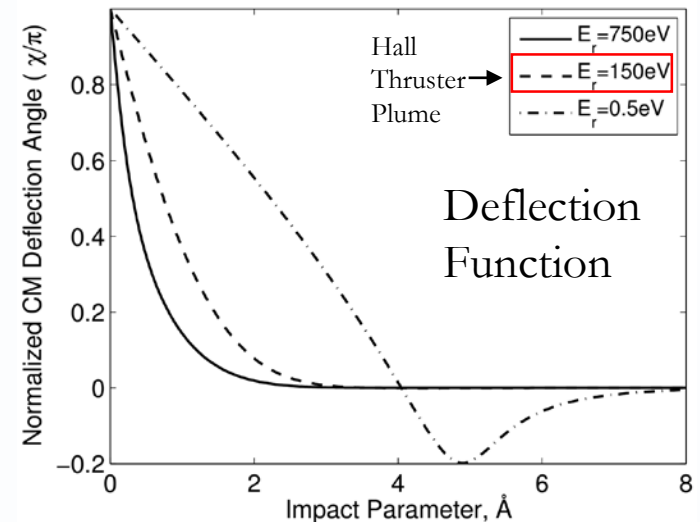
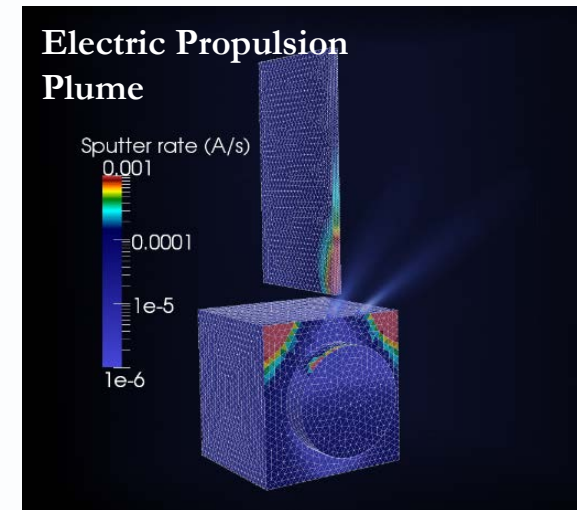


U.S. AIR FORCE



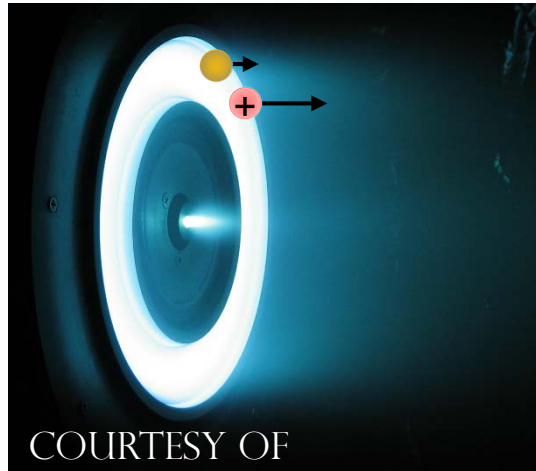


- Introduction
- Method
 - Classical approach with quantum potential
 - Table lookup of scattering angles
 - Effective elastic cross-section
 - Implementation
- Performance Study
- Conclusion

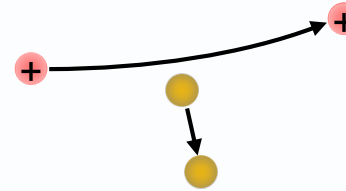




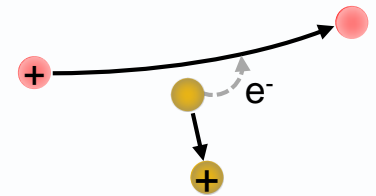
- + Beam ion
- + CEX ion
- High energy atom
- Thermal atom



Momentum Exchange (MEX)

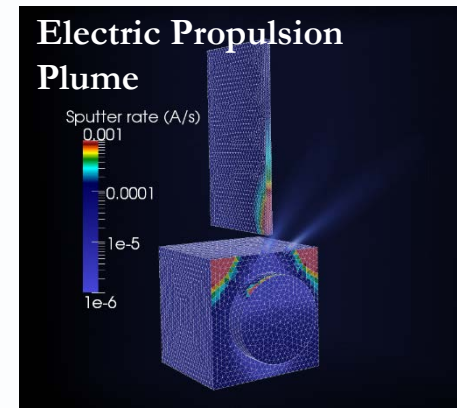


Charge Exchange (CEX)



Motivation

- Important for EP plume simulations
 - Accurate plume profile
 - Assess spacecraft-plume interaction
- Even a reduced model takes up >10% of overall plume simulation time



Objective

- Accurate and fast method for elastic collisions between high energy beam ions and slow neutral atoms



- **Simple model¹**
 - MEX: Variable hard sphere model with isotropic scattering
 - CEX: No momentum transfer
- **High fidelity model²⁻⁴**
 - Classical scattering with *ab initio* potential
 - Exchange charge depending of charge exchange probability ($P_{\text{CEX}}=0.5^{2,3}$, or numerically evaluated P_{CEX}^4)
- **Reduced model^{5,6}**
 - Sample from curve-fit representation of differential cross-section at a given energy

[1] D. Oh, Ph.D. thesis, Massachusetts Institute of Technology, Cambridge, MA 1997.

[2] I. Mikellides, I. Katz, R. Kuharski, and M. Mandell, *Journal of Propulsion and Power* **21**, 111–118 (2005).

[3] I. D. Boyd and R. A. Dressler, *Journal of Applied Physics* **92**, 1764–1774 (2002).

[4] S. J. Araki and R. E. Wirz, *IEEE Transactions on Plasma Science* **41** (2013).

[5] M. K. Scharfe, J. W. Koo, and G. Azamia, *AIP Conference Proceedings*, Vol. 1333 (AIP, 2011), pp. 1085–1090.

[6] P. N. Giuliano and I. D. Boyd, *Physics of Plasmas* **20** (2013).



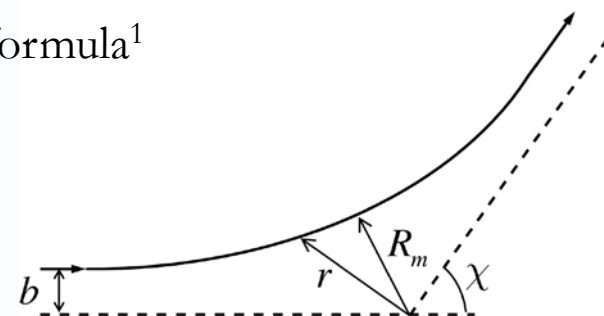
Classical Scattering Model



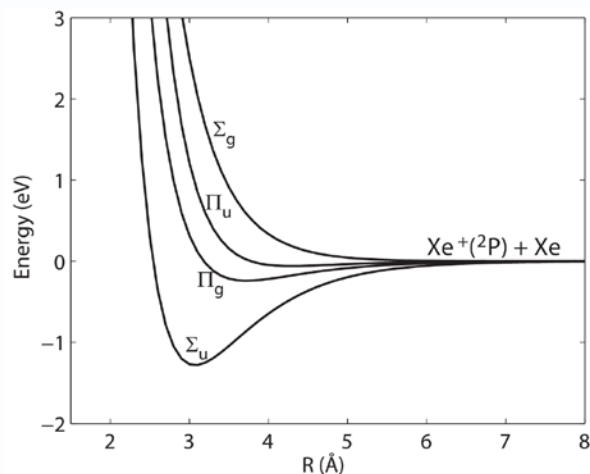
$$\chi(b, E_r) = \pi - 2b \int_{R_m(b, E_r)}^{\infty} \frac{dr}{r^2 [1 - b^2 / r^2 - V(r) / E_r]^{1/2}}$$

$$\approx \pi - 2b \frac{\pi}{nR_m} \sum_{j=1}^{n/2} f(v_j) \quad \text{Gauss-Mehler's formula}^1$$

$$v_j = \cos \frac{2j-1}{2n} \pi, \quad f(v_j) = \left[\frac{1 - v_j^2}{1 - V(R_m / v_j) - b^2 v_j^2 / R_m^2} \right]^{1/2}$$



Xe⁺ + Xe Spin-Orbit Free Potential



1. Fitting potential pair into Morse potential form

$$V_{avg}(r) = D_e (e^{2b(r_e - r)} - 2e^{b(r_e - r)})$$

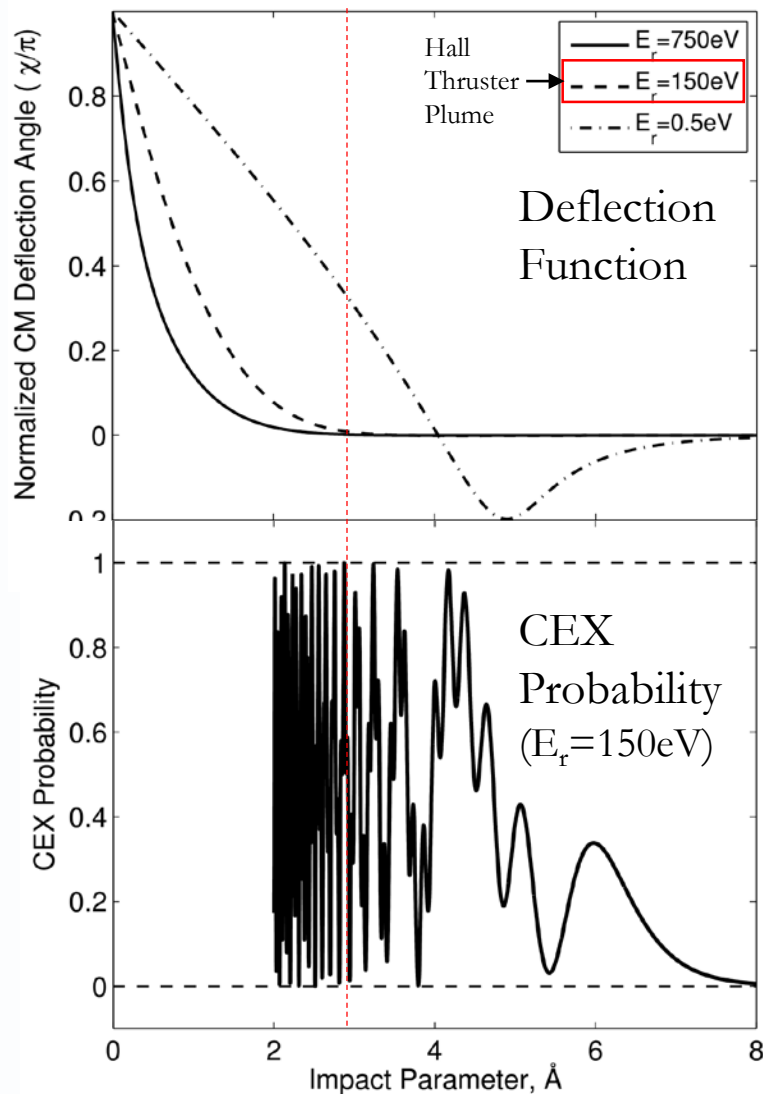
2. Apply statistical weights

$$V(r) = \frac{1}{3} V_{\Sigma, avg}(r) + \frac{2}{3} V_{\Pi, avg}(r)$$

[1] F. J. Smith, Physica **30**, 497-504 (1964).



Xe⁺+Xe Deflection Function



Deflection angle is mostly affected by repulsive potential

- Monotonically decreasing function
- Large angle at short range
- Small angle at long range

CEX Probability

$$P_{CEX}(b) = \frac{1}{3} \sin^2 \Delta\eta_{\Sigma} + \frac{2}{3} \sin^2 \Delta\eta_{\Pi}$$

$$\Delta\eta = -\frac{m_r}{\hbar^2 k} \int_{R_m}^{\infty} \frac{\Delta V(r) dr}{[1 - R_m^2 / r^2]^{1/2}}$$

- Highly oscillatory at small impact parameters ($P_{CEX}=0.5$)
- No deflection when P_{CEX} has some feature



Total and Differential Cross-Section



- Charge exchange cross-section¹

$$\sigma_{CEX} = 87.3 - 13.6 \log(E)$$

- Effective elastic cross-section

- Indication of when a significant momentum exchange occurs
- Corresponds to a cut-off impact parameter

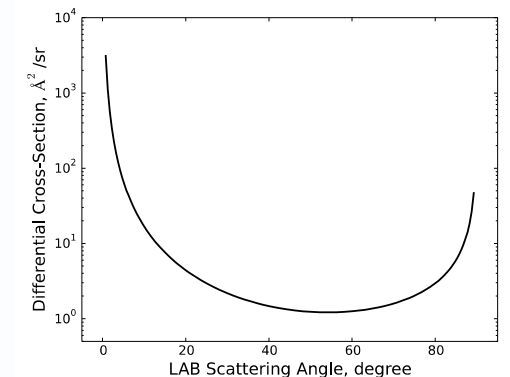
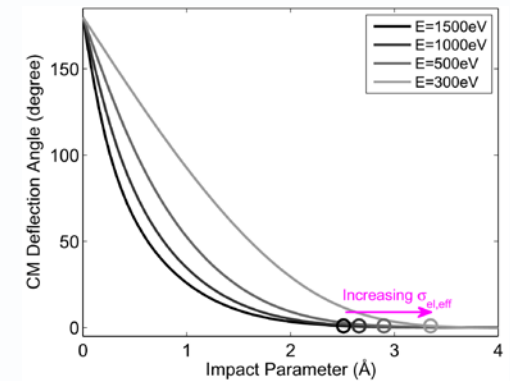
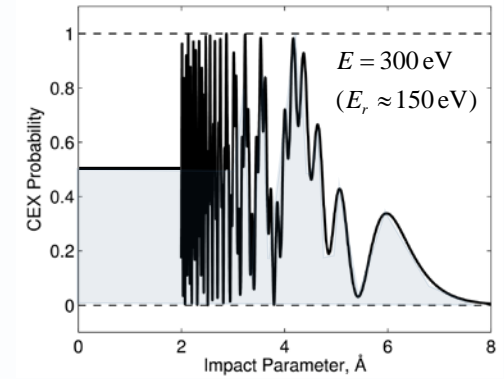
$$\sigma_{el} = 62.3 - 13.4 \log(E)$$

- Differential cross-section

$$I_{CM}(\chi, E_r) = \frac{d\sigma(\chi)}{d\Omega} \Big|_{CM} = \left| \frac{b}{\sin \chi (d\chi/db)} \right|$$

$$I_{CM}'(\chi) = (1 - P_{CEX}(\chi)) I_{CM}(\chi) + P_{CEX} I_{CM}(\pi - \chi)$$

Transformation to LAB frame



[1] J. S. Miller, S. H. Pullins, D. J. Levandier, Y.-H. Chiu, and R. A. Dressler, Journal of Applied Physics 91, 984-991 (2002).



Formulation of a Lookup Table

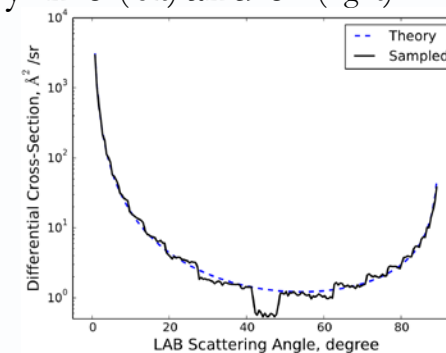
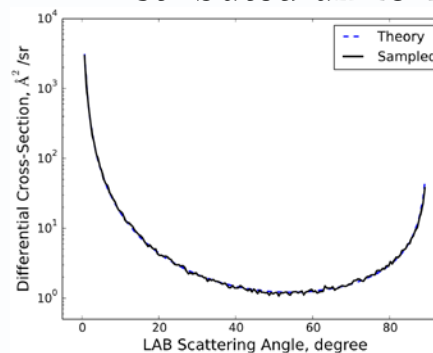


- Determine scattering angle $\chi(E_r, b)$ for every collision pair
 - Solving classical scattering equation is slow
 - Use a lookup table and interpolate to collision pair's relative energy and impact parameter
1. User defined parameters $E_{min}, E_{max}, N_E,$ and N_b
 2. Get max impact parameter from $b_{max}(E_r) = \sqrt{\sigma_{el}(E_r) / \pi}$
 3. Solve χ at discrete b and E values

$$E_j = E_{min} + j \frac{E_{max} - E_{min}}{N_E - 1}, \quad 0 \leq j \leq N_E - 1$$

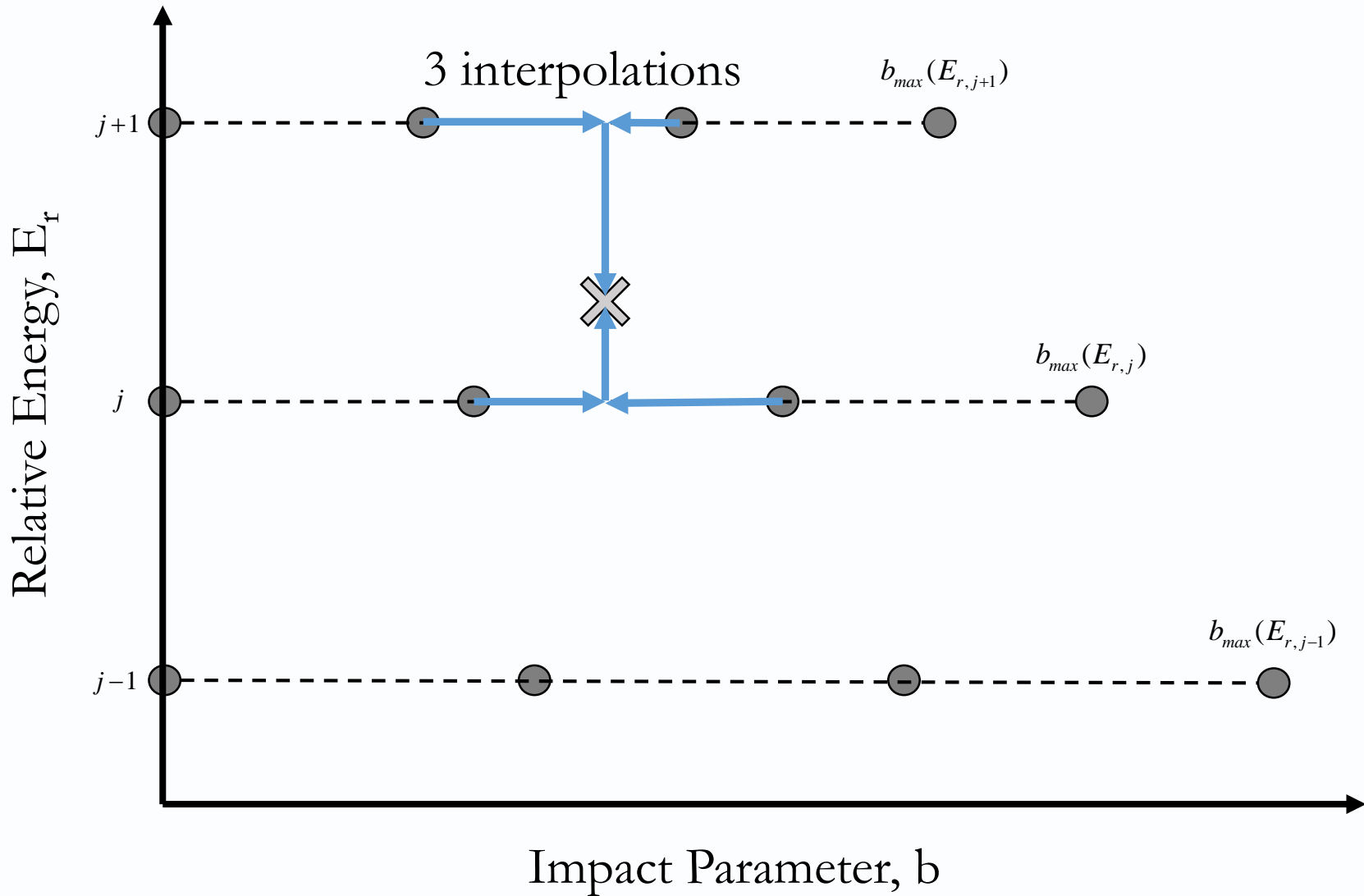
$$b_i = i \frac{b_{max}}{N_b - 1}, \quad 0 \leq i \leq N_b - 1$$

Distributed uniformly in b (left) and b^2 (right)





Using a Lookup Table





Implementation in MCC Method



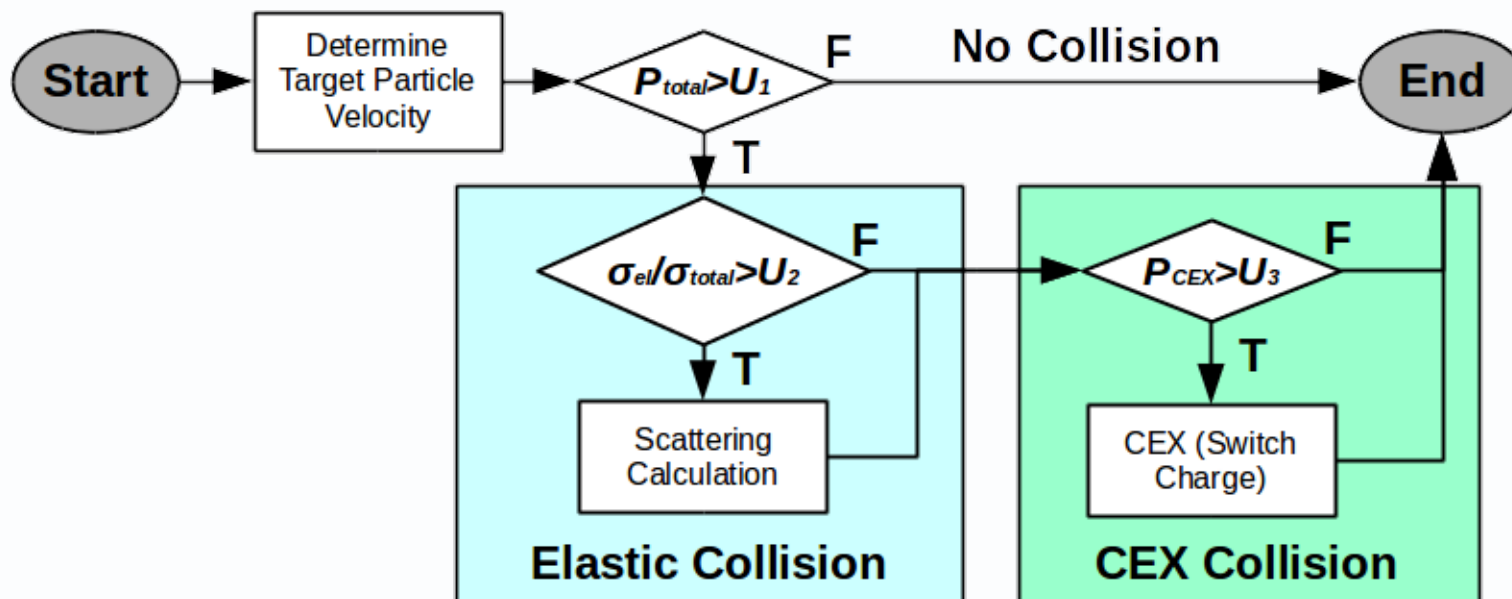
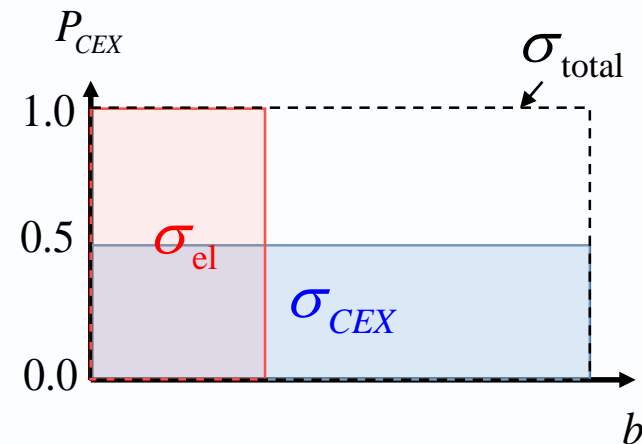
- Total elastic collision cross-section

$$\sigma_{\text{total}} = 2\sigma_{\text{CEX}}$$

$$\Rightarrow P_{\text{total}} = 1 - \exp(-\gamma n_0 \sigma_{\text{total}} v_{\text{rel}} \Delta t)$$

- Charge exchange probability

$$P_{\text{CEX}} = 0.5$$





Further Improvement is Possible

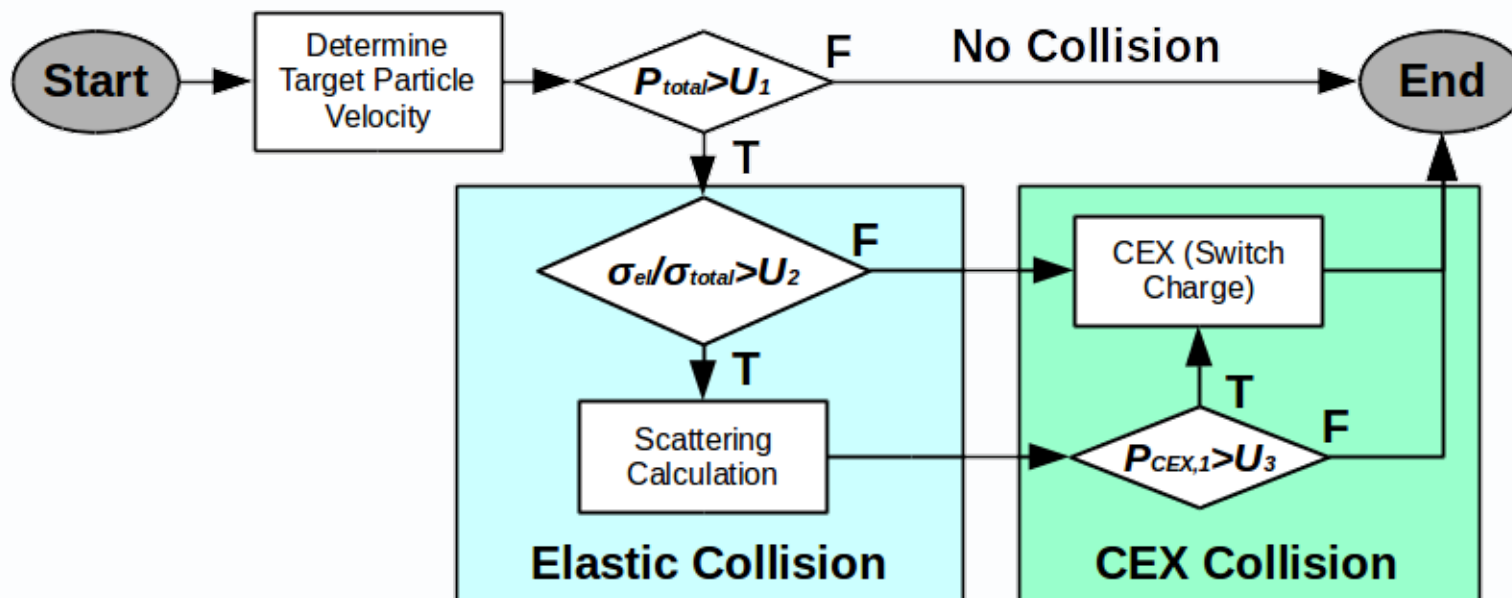
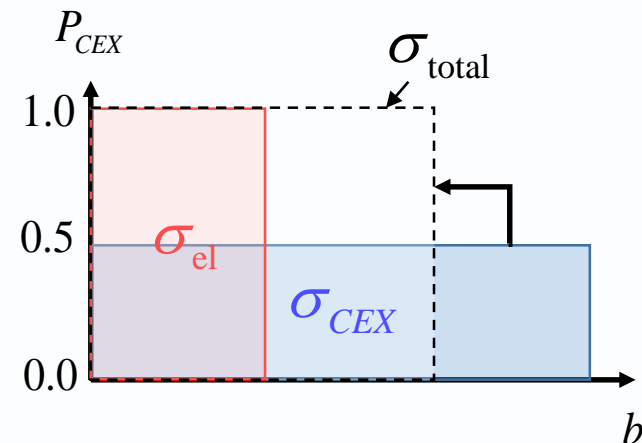


- Total elastic collision cross-section

$$\sigma_{\text{total}} = \sigma_{\text{CEX}} + 0.5\sigma_{\text{el}}$$

- Charge exchange probability

$$P_{\text{CEX},1} = 0.5 \text{ and } P_{\text{CEX},2} = 1.0$$





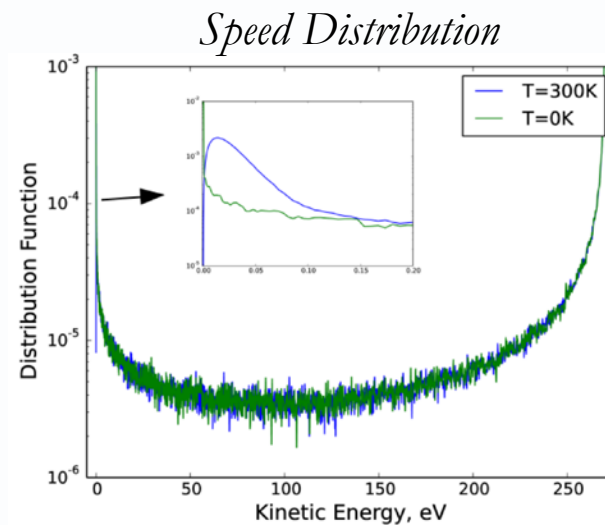
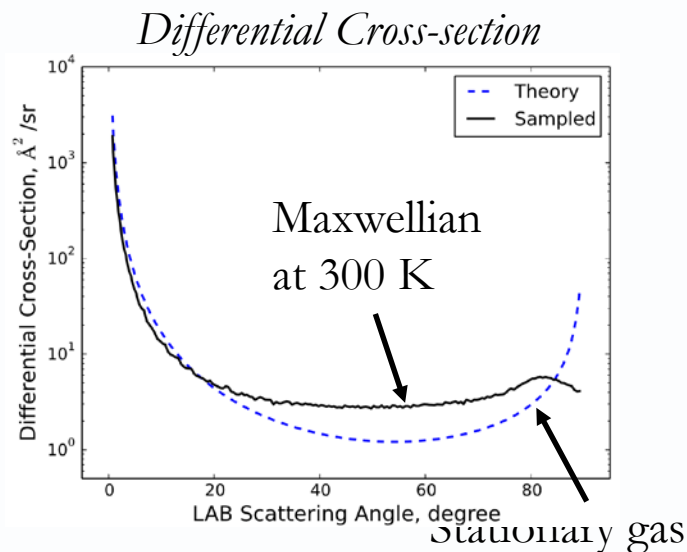
- Apply collisions to 1,146,700 particles injected at 270 eV (19,920 m/s)
- Repeat calculations for 100 times
- Only reported collision calculation time
- Baseline: reduced model based on differential cross-section for 270 eV LAB energy ions

Model	Wall Time (s)	% Baseline
Baseline (Sampling from curve-fit to differential σ)	61.67	100.0
(1) Lookup Table	45.75	74.2
(2) Effective Elastic Collision $\sigma + (1)$	36.21	58.7
(3) Stationary Background Gas + (2)	17.63	38.6



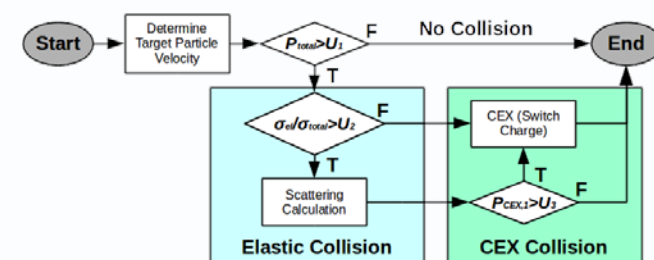
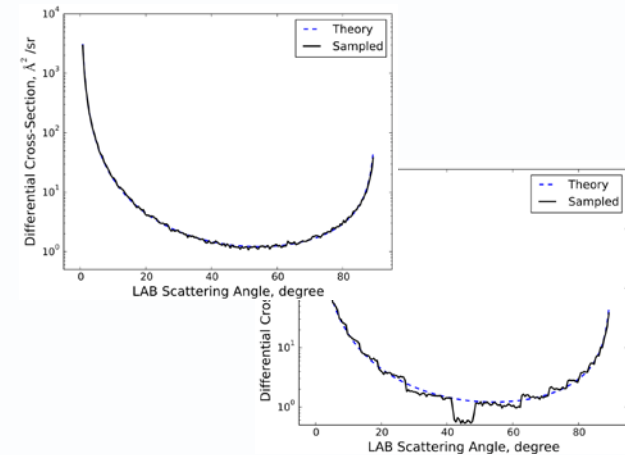
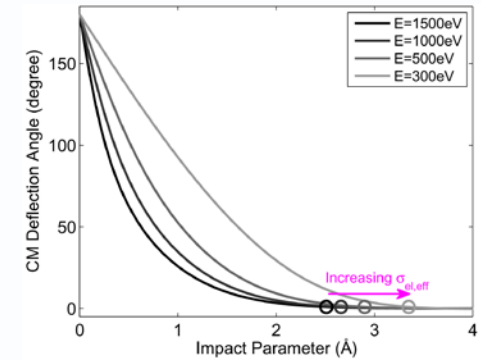
Does the assumption made to pre-collision neutral velocity have any significant effect to the plume simulation?

- Differential cross-section is altered significantly
 - Especially the large angle scattered population
- This population only has small energy ($<0.2\text{eV}$)





- Acceleration of elastic collision calculation without losing accuracy from high-fidelity model
 - Effective elastic collision cross-section
 - Formulation of a lookup table
 - Uniformly distributed E and b
 - Implementation with based on three different cross-sections
- Stationary background gas assumption is sufficient for plume simulations
- >70% improvement in speed compared to a reduced model





Thank you